Coastal Engineering 189 (2024) 104458

Contents lists available at ScienceDirect

Coastal Engineering

journal homepage: www.elsevier.com/locate/coastaleng

Short communication

Satellite-derived bathymetry from correlation of Sentinel-2 spectral bands to derive wave kinematics: Qualification of Sentinel-2 S2Shores estimates with hydrographic standards

Rafael Almar [a,*], Erwin W.J. Bergsma [b], Grégoire Thoumyre [a], Lemai-Chenevier Solange [b], Sophie Loyer [c], Stephanie Artigues [b], Grégoire Salles [a], Thierry Garlan [c], Anne Lifermann [b]

[a] LEGOS (Univ. Toulouse, CNRS, CNES, IRD), 14, av. Edouard Belin, Toulouse, 31400, France
[b] CNES, 18, av. Edouard Belin, Toulouse, 31400, France
[c] Service Hydrographique et Océanographique de la Marine (Shom), 13 rue du Chatellier, Brest, 29240, France

ARTICLE INFO

Keywords:
Optical imagery
S2Shores
Satellite to shores
Satellite-derived bathymetry
Aquitain atlantic coast
France

ABSTRACT

There is a pressing need for a fast and efficient satellite remote sensing tool to estimate coastal bathymetry for any coastline in the world. To date, satellite methods for deriving bathymetry have mainly focused on linking the radiometric response to a known water depth, as with SPOT, Landsat and Sentinel. Here, wave properties (static and dynamic) are approximated using the small time delay between the different color bands of Sentinel-2 to then calculate a depth using wave linear dispersion theory. In this paper, we present a spatial correlation method within the S2Shores (Satellites to Shores) Python toolbox: a processing chain/toolbox of coastal observations using methods applied to optical satellites. The resulting individual bathymetries are finally qualified according to the standards of the International Hydrographic Organization, anticipating their operational use.

1. Introduction

The current lack of information on coastal water depths can be linked to major technological and scientific barriers that lead to unacceptable uncertainties in civilian (coastal management, structures, crisis management, natural hazards, coastal vulnerability — sea state and erosion/flooding forecasting) and military (projection of amphibious operations, sea state forecasting) domains. Hydrographic services such as the Service Hydrographique et Oceanographique de la Marine (Shom) in France or the UK Hydrographic Office (UKHO) in the United Kingdom survey less than 1% of their continental shelf each year, which means that surveys are repeated over several years, not to mention that some areas remain unsurveyed or the bathymetric information is decades old. Traditional survey campaigns using high-resolution multibeam sounders or more recent lidar surveys cover no more than a few thousandths of the world's very shallow waters. Given this, and the high variability of these environments, the validity of these surveys is questionable. Fast, inexpensive, and efficient methods are particularly needed for studies of seafloor variability such as that experienced at estuaries, channels, and features such as submarine sand dunes (Daly et al., 2022). This need is even more important for areas made inaccessible by conflicts, too far from base ports, or too infrequently visited by ships to be surveyed (Laporte et al., 2020; Cesbron et al., 2021).

This data gap, which limits society's ability to respond to today's emerging questions about the coastal environment, creates an immediate need for satellite remote sensing tools, for example to estimate coastal bathymetry anywhere in the world (Benveniste et al., 2019; Melet et al., 2020). In the 2016 market report (Copernicus Market Report, 2016), trends extrapolated from the state of the remote sensing-based market in 2015 clearly show its development and emergence. There are no figures yet for bathymetry alone, but this study shows that the market is growing and is far from being mature and saturated. Moreover, this study was limited to the market generated by the satellite data collection in the framework of Copernicus (10 m resolution) and did not take into account the market offered by very high resolution (Pleiades, WorldView...etc.), nor the extension of the validity of the method to 50 m or even 80 m depth. The estimated cost of producing bathymetry from Sentinel-2 is estimated at between 90 and 95 € per km^2, which represents a 10-foldreduction compared to the cost of production by LIDAR technology in shallow areas. A technology watch showed that commercial satellite bathymetry products currently only offer products for shallow waters (0–20 m for clear waters, 0–5 m for turbid waters (Cesbron et al., 2021)). This information can be addressed to several markets and sectors of activity, including the

* Corresponding author.
E-mail address: rafael.almar@ird.fr (R. Almar).

https://doi.org/10.1016/j.coastaleng.2024.104458
Received 20 June 2023; Received in revised form 15 December 2023; Accepted 10 January 2024
Available online 12 January 2024

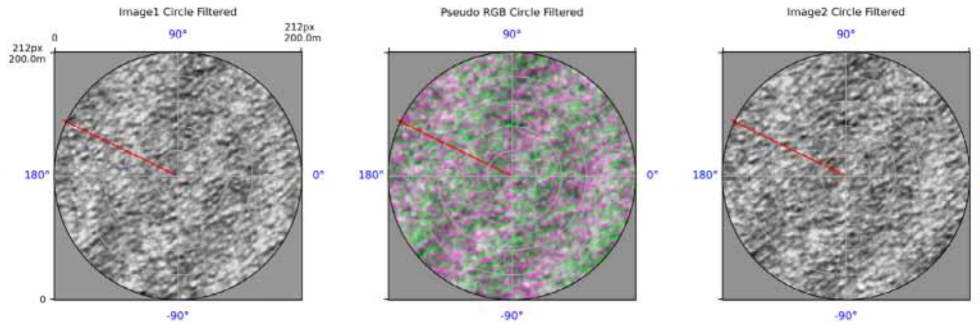

Fig. 1. Example of B02 (left) and B04 bands (right). The difference shows the propagation of swell waves within their main direction of propagation (red arrow), superimposed with wind waves of much shorter wavelength.

marine renewable energy industry, the offshore oil and gas sector, the maritime transport sector, environmental scientific studies, etc.

Satellite methods have mainly focused on bathymetry by inversion of radiometry from satellites such as SPOT and Landsat (Lyzenga et al., 2006; Caballero and Stumpf, 2020, 2023). When dealing with optical measurements of ocean waves, spectral approaches (through Fourier and wavelet analysis) generally hold the line with dense and long temporal (Holman and Bergsma, 2021) or spatial (Bergsma et al., 2019b, 2021) datasets, typically several periods and wavelengths respectively. However, in contrast to shore-based video cameras or drone surveys, satellite data tend to be sparse in time and generally have lower spatial resolution (Bergsma and Almar, 2020), leading to an intrinsic limitation in output resolution. Correlation approaches have been previously evaluated to capture wave kinematics from video (Bergsma and Almar, 2018; Almar et al., 2009; Abessolo et al., 2020) and satellite (Almar et al., 2019, 2022). Sensitivity analysis suggests that such approaches become advantageous over spectral methods for time- or space-limited computational windows for the need for a high-resolution spatial approach in shallow water when the computational time or space window is as small as a wave period or wavelength.

It is also essential to qualify the satellite estimates to facilitate their use. The International Hydrographic Organization (IHO) standards are the most widely used bathymetric reference recognized by hydrographic organizations. Regardless of the accuracy of the estimates, which currently range from sub-metric to multi-metric values, it is essential to qualify these data. However, these standards were developed for surveying and do not always apply to satellite-derived bathymetry. Despite an increasing number of attempts to qualify such satellite products (Laporte and Coulibaly, 2019; Matsumoto, 2016; Kurniawan et al., 2021; Caballero and Stumpf, 2020; Mavraeidopoulos et al., 2017), there is still a need to adopt common multi-source standards.

Here, satellite-derived bathymetry is produced from wave kinematics using Sentinel-2 at a documented site, the Gironde estuary area, in the Bay of Bicay (South West Atlantic coast of France, Europe). A spatial correlation approach is introduced and applied, following the S2Shores (Satellites to Shores) framework (Baba et al., 2021; Daly et al., 2022; Bergsma et al., 2019b; Almar et al., 2021b), developed to facilitate the use of satellites for the coastal zone.

2. Methodology

2.1. Sentinel-2 images and validation dataset

Sentinel-2 sensors collect spectral bands with a slight time delay between each of the spectral bands (Binet et al., 2022a). Taking advantage of this artifact, several studies estimate waves, currents and finally inverse bathymetry (Yurovskaya et al., 2019; Kudryavtsev et al., 2017; Bergsma et al., 2021; Almar et al., 2019). Considering the bands with 10 meter resolution (blue : B02, near infrared : B08, green : B03 and red : B04), a maximum delay of 1.005 s can be found between the blue and red bands (Fig. 4) in the ESA User's Handbook (Sentinel, 2015) (see Fig. 1), are reported in the Table 1. These constants are averages over all existing Sentinel-2 orbits and are not fully representative on a global scale. Using Sentinel-2 publicly available data, these time delays have been reprocessed and are given as a function of satellite S2-A and B, and latitude (Binet et al., 2022a).

Table 1
Δt per bands given in the ESA S2 Users handbook. B02 is used as the reference t = 0 s.

	B02	B08	B03	B04
Δt [s]	0	0.264	0.527	1.005

Table 2
Images dates and corresponding wave parameters (tide, significant wave height (Hs), peak period (Tp) and direction) at the moment of acquisition, from ERA 5 (ECMWF).

Satellite	Tide (m)	Hs (m)	Tp (s)	Direction (°)
S2A 2018-05-04	−1.179	1.775	11.55	304
S2A 2018-08-02	−0.851	1.471	11.03	302
S2A 2020-06-22	−1.432	1.927	11.44	286
S2B 2020-07-07	−1.698	1.634	10.97	303

In order to test the performance of the spatial correlation method, the area around the Gironde estuary in France (see Fig. 2) has been selected because of the presence of several morphological features; open sandy beaches exposed to waves, tidal sandbars and a continental shelf with a weak slope (depths reaching only 50 m 25 km from the coast). Considering the presence of recurrent maritime activities in the area, the bathymetry of the Shom is well known, giving us the opportunity to confront our results with a verified and certified dataset.

The reference bathymetric survey used here is EMOdnet (Thierry et al., 2019) with a resolution of about 115 m. The surveys are performed according to IHO S-44 standards. The vertical accuracy of the product is less than 1% and meets the highest S-44 order standards Appendix A.

Four single-date satellite estimates with arbitrary a priori good conditions (i.e. clear sky, presence of waves, and signal coherence close to good in summer with sufficient light) are qualified. The comparison covers a 100 km × 100 km region around the Gironde estuary and corresponds to the Sentinel-2 orbit R094, tile 30TXR (UTM code associated with each tile, for more information, visit https://sentinel.esa.int/web/sentinel/missions/sentinel-2/data-products). The method works indifferently for publicly available data, Level-1C (Top-of-atmosphere reflectances in cartographic geometry) but also Level-2A (Atmospherically corrected Surface Reflectances in cartographic geometry). The data used in the composite are listed in the Table 2 along with their wave and tide conditions.

2.2. Bathymetry inversion from waves: a correlation approach

S2Shores is a Python library designed for deriving wave field characteristics and estimating bathymetry using sparse temporal satellite

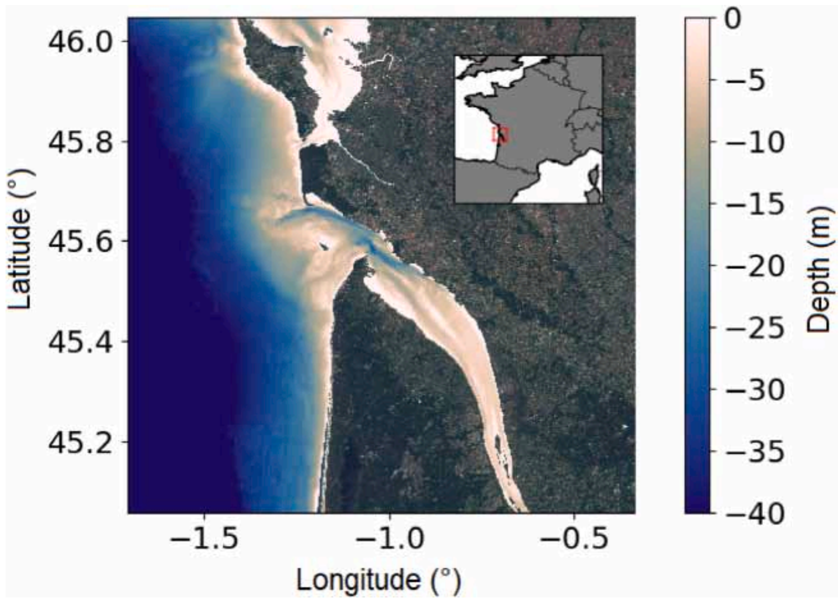

Fig. 2. Sentinel-2 30TXR tile footprint at the Gironde estuary, South West Atlantic coast of France (Nouvelle Aquitaine Region). Emodnet bathymetry in color for the sea part, superimposed with Sentinel-2 true color image for terrestrial part.

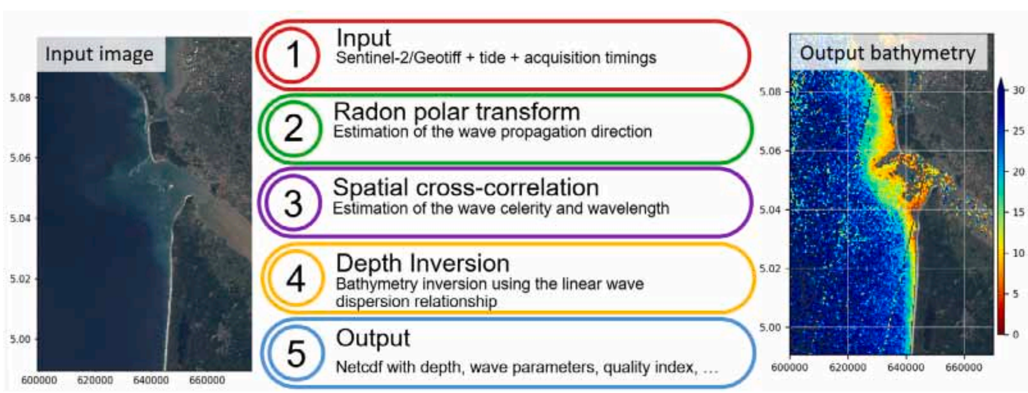

Fig. 3. Sketch of the S2Shores framework from initial satellite image to derived bathymetry.

optical data (Fig. 3). However, it is not limited to satellite use and can be applied to shore-based video camera systems and UAVs (Bergsma et al., 2022; Thoumyre et al., 2023). The library's structure facilitates image processing, wave geometry and motion detection, and depth retrieval through inversion. The code is designed to be agile, allowing flexibility in input, processing, and potential outputs beyond depth estimation. The library includes three methods for estimating wave characteristics, each focusing on different measurements such as spatial displacement, spectral phase shift, and temporal reconstruction of local time series. The object-oriented structure allows for homogenization and streamlined code. The time delay for calculations is obtained from raw satellite information, and the library aims to solve equations based on measurements, considering factors like roll, yaw, pitch, and position. The text emphasizes the challenges of deducing wave period directly from sparse temporal data and highlights the suitability of the library for various sensor types beyond optical and radar.

Here we introduce one of the methods implemented so far (temporal correlation (Almar et al., 2019), spatial–spectral (Bergsma et al., 2019b)) within this S2Shores framework (Fig. 3), and based on spatial correlation.

The underlying bathymetry dictates the wave celerity and wavelength in the case of waves propagating through intermediate to shallow water. The limits for intermediate and shallow waters are wavelength dependent, with $h_{int} = \frac{\lambda}{2}$ and $h_{sh} = \frac{\lambda}{20}$ being the commonly accepted limits for shallow (h_{int}) and intermediate (h_{int}) water depths. Thus, from intermediate depths to the coast, the linear dispersion relation (1) can be used to estimate a local depth.

$$c^2 = \frac{g}{k}\tanh(kh) \Leftrightarrow h = \frac{\tanh^{-1}\left(\frac{c^2 k}{g}\right)}{k} \tag{1}$$

where c is the wave celerity, g the gravitational acceleration constant, h the water depth and k the wavenumber (inverse of the wavelength $k = 1/L$).

Thus, two parameters between celerity, wavelength λ ($\frac{1}{k}$), wave frequency ω and period T ($\frac{1}{\omega}$) must be known to solve Eq. (1). Due to the dominance of spatial information over temporal information in Sentinel-2 products (Bergsma et al., 2021), the celerity-wavelength pair is solved here (Almar et al., 2022).

Previous studies have shown that the polar Radon transform (RT) is particularly efficient in capturing the wave direction (Almar et al., 2014, 2019; Bergsma et al., 2019b, 2021). Here, we use the same computational framework in which the RT is used to extract the wave signal along the main direction of propagation for each band used (Fig. 4). The RT integrates the pixel intensity ($I(x, y)$) along lines defined by angle θ and radius ρ (2):

$$R_I(\theta, \rho) = \int I(x, y)\delta(\rho - x cos(\theta) - y sin(\theta)) dx dy \tag{2}$$

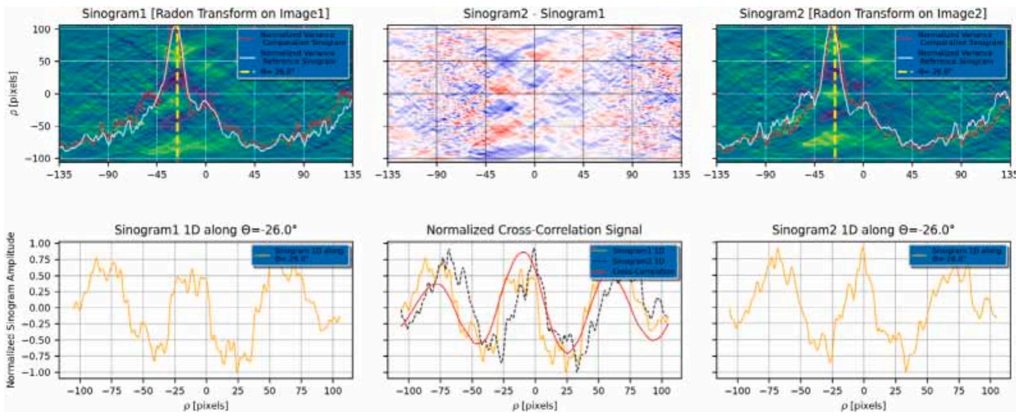

Fig. 4. Upper line shows the polar sinograms from applying the Radon transform on the computing windows in B02 (left) and B04 (right) (Fig. 4). Lower line shows the signals over the direction of the maximum of variance. Central panel indicates the resulting cross-correlation between bands.

With δ the Dirac function, R_I the sinogram, the signal per direction θ over the associated ray of length ρ. The angular limits of Eq. (2) are set to $0° > \theta > 180°$. By integrating along the lines, the RT accentuates linear features and thus acts as a low pass filter, enhancing swell waves and reducing high frequency sensor noise and short crested wind waves.

The derivation of the RT differs from the previously mentioned approaches. After calculating the sinogram by direction θ, the most dominant wave propagation angle is found by the maximum variance on the rays ρ. This is illustrated in Fig. 4, the main peak is observed at 45°, which corresponds to the presented case. In the dominant direction, a cross-correlation is used to estimate the spatial offset Δx between the two signals (in this case Sentinel-2, bands 2 and 4). Given the known time delay Δt between the two bands, a celerity (c) is computed as $c = \frac{\Delta x}{\Delta t}$. The dominant wavelength L is estimated by a zero crossing method applied to the covariant signal between the two series.

The celerity of coastal waves is on the order of 1 to 10 m/s. Because of the short time lag (~1 s) between Sentinel-2 images and their resolution (10 m), it is virtually impossible to measure coastal wave propagation without increasing the resolution. This would mean a spatial lag of either 1 pixel or less. This is addressed by linearly re-sampling the angular rays extracted from the sinograms to a resolution of 1 m.

3. Results

Estimates at different single dates are shown in Fig. 5. The correlations, which range from 0.45 to 0.71, show that the regional pattern is well captured. However, the data are scattered, as reflected by relatively large RMSE values, here from 12.37 m to 16.36 m. Interestingly, the bias increases with depth. These observations tend to show that intermediate waters are better estimated than deeper ones, while the method tends to overestimate depth in the shallowest waters. The deep water saturation (deviation from the 1:1 line) varies with the environmental conditions experienced during each acquisition and the geometry, conditioning the way waves are sensed (Almar et al., 2021a; Kudryavtsev et al., 2017; Cox and Munk, 1954).

The Pertuis d'Antioche, sheltered by the island of Oléron, with potentially less swell compared to open water and more wind waves limited by the fetch, shows reasonable results overall. At the mouth of the Gironde, which has a complex bathymetry and therefore complex wave shapes (with a cross-sea due to refraction), the S2Shores capture the main channels. Similarly, the Cordouan tidal bank is overestimated but remains visible.

Each of the S2Shores estimates was classified according to the 4 major orders of the S-44 (Appendix A). This classification is based on the vertical difference between the S2Shores estimates and the reference surface at each grid cell. The evaluation was performed on 10 m bathymetric slices to detect possible differences in performance between depth ranges. As a reminder, the orders used for this classification are specific to hydrographic surveys dedicated to navigation safety and for which a correspondence exists with the CATegory Zone Of Confidence (CATZOC) classification (Appendix B). This qualification remains a reference in the field of hydrography, but in the long term the objective is to be able to classify satellite-derived bathymetry surveys in the specification matrix of Edition 6, as some pioneering studies already initiated with color-based methods (Chénier et al., 2019; Pike et al., 2019; Nicolas et al., 2023; Cahalane et al., 2019). The proportion of S2Shores bathymetry estimates that can be classified reaches 20% for depths less than 30 m and 10% or less for deeper waters.

4. Discussion

4.1. Limitations and range of applicability

In the long run, qualified S2Shores estimates allow a gradual reduction of areas that have not been surveyed recently (i.e., less than 20 years). The delivered product seems to be less reliable in very shallow waters (overestimation) and in deep waters (underestimation). Waves are increasingly non-linear while they propagate shoreward (Tissier et al., 2011) and reach shallow waters. There is a link between wave skewness, non-linearity and depth estimation error with the limits of the linear dispersion relation (Bergsma and Almar, 2018). Beyond these physical considerations, a residual sensing error is also linked to method-based parameters and a changing wave shape as incident waves propagate inshore. In deep waters the underestimation can be associated with the modulation transfer function between pixel intensity and surface elevation (Holman et al., 2017; Bergsma et al., 2019a) which, uncorrected, favors the derivative of the surface rather than the surface itself (Almar et al., 2021a). As a result, short wavelength have more weight which artificially reduce the deep water limit of the method applicability compared to theory (Bergsma and Almar, 2020)

4.2. Image quality, pre-selection and multi-date compositing

In this study are presented some of the best data, i.e. without clouds and waves and with favorable relative waves, view and sun geometry. A few parameters affect the quality of wave-based inversion methods from satellites. These are explored in Almar et al. (2021b), and among the wave parameters, the relative direction to the orbit is identified as critical, as vertical crests cannot be seen optically (Almar et al., 2021a). Sun elevation and luminosity in general seem to be key: the brighter

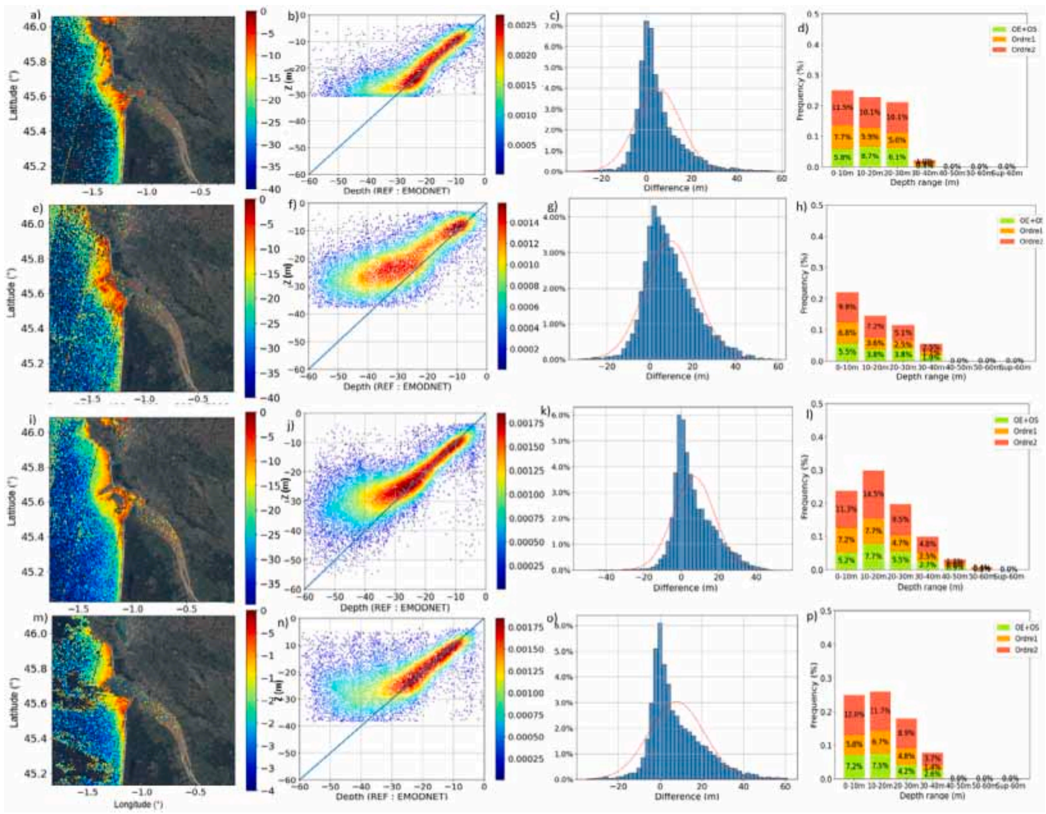

Fig. 5. First column: S2Shores estimates. Second column: S2Shores estimates versus Emodnet reference survey (Fig. 2). Third column: distribution of error on estimates. The OO values correspond to the probes not respecting any of the defined orders. Fourth column: distribution of estimates within the IHO norm S-44 (vertical uncertainty). Lines stand for the dates in Table 1: 2018-05-04, 2018-08-02, 2020-06-22 and 2020-07-07.

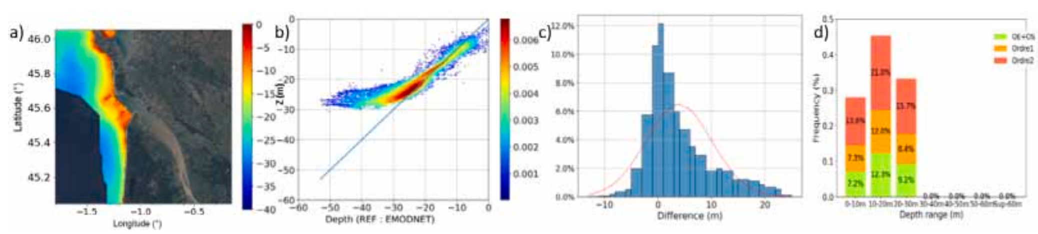

Fig. 6. (a) S2Shores multi-date composite estimate. (b) S2Shores estimate versus Emodnet reference survey (Fig. 2). (c) distribution of error on estimate. The OO values correspond to the probes not respecting any of the defined orders. (d) distribution of estimate within the IHO norm S-44 (vertical uncertainty). Composite generated using the dates in Table 1: 2018-05-04, 2018-08-02, 2020-06-22 and 2020-07-07 and described in Fig. 5. A multi-date dispersion is used to remove spurious estimate offshore.

the better, as low values increase the noise (Kudryavtsev et al., 2017; Cox and Munk, 1954).

As such, the bathymetry estimation benefits from incorporating smoothing techniques to minimize errors and estimating confidence intervals. These considerations are crucial for enhancing operational effectiveness.

Temporal aggregation of multiple dates is a simple way to improve the reliability of bathymetry estimates (Almar et al., 2021b; Baba et al., 2021; Daly et al., 2022). This is possible with the revisit of satellites such as Sentinel-2. After merging different date estimates, the use of a maximum variance threshold allows to refine the confidence region before a final smoothing of the estimated depth with an adaptive kernel size based on depth. Compositing strengthens the robustness of the estimates, from individuals that are fairly noisy, with composite patterns clearer and smoother (Fig. 6) and improved RMSE value down to 7.2 m. Besides a simple averaging or median, several ways are explored, such as weighted by noise (Daly et al., 2022; Almar et al., 2021b), wave period and using tide estimation as a quality proxy for the bathymetry (Thuan et al., 2019).

4.3. *Multi pairs of band*

Here, we do not make full use of the information contained in the Sentinel-2 spectral bands. The celerity estimation could potentially be made more robust by increasing the number of band pairs used and aggregating them, as done in the temporal correlation method (Almar et al., 2019, 2022). Beyond the 10 m resolution bands, this could also be done by including the 20 m bands resampled over the same 1 m polar grid. The use of these bands would result in 28 pairs, over a longer duration (up to 2.586 s between B09/B02), potentially reducing the errors in wave detection. Advantages can be obtained by estimating celerity through multi-band linear regression compared to using a single pair of bands. While the use of linear regression potentially improve the robustness, it also adds substantial noise as the best pair is always B02/B04, because of dt between pairs which is maximum and spectral considerations. Overall, the gain is very small compared with the computing time which is multiplied by 28 compared with the optimal single pair estimate. For this reason we prefer to discard this multi-pair linear regression approach for now.

4.4. Sensitivity of the method to the resolution in space, time and computation window

Only a few settings need to be specified for the method to estimate wave parameters and subsequently determine the depth. As long as L≫dx, wavelength estimation appears to be rather insensitive to the spatial resolution. The estimation of the wavelength has also independence from the temporal lag between two snapshots. In contrast, celerity estimation is closely tied to the temporal resolution and also yields improved results with higher resolution. By nature (C = dx/dt), celerity estimate shows a high sensitivity to spatio-temporal resolution, even if the Radon Transform resolution augmentation reduces the spatial resolution influence (Bergsma et al., 2019b). However, spatio-temporal resolution cannot be changed and is given by the technical specifications of the mission and the only arbitrary setting pertains to the size of the computation window, here measuring 800 × 800 m (80 × 80 pixels) to deal with the reasonable longest wavelengths possibly observed. The size of the computational window has a direct impact on both celerity and wavelength. Although the correlation approach potentially allows for a smaller domain than a spectral approach (Bergsma et al., 2021), which typically requires multiple wavelengths, it provides stabilization when passing a wavelength. In shallow water, waves shoal and become skewed (Tissier et al., 2011; Almar et al., 2014), allowing for less than a wavelength calculation window for resolving celerity. In general, celerity estimation errors decrease as the temporal and spatial resolution and the length of the signal (relative to the period or wavelength) increase (Almar et al., 2020), which encourages the use of on-demand satellite video (Almar et al., 2022; Cesbron et al., 2021).

4.5. Timing correction

The importance of the accuracy of the timing value between spectral bands depends on the variable under consideration, and accurate timing estimation is essential for accurate celerity estimation. This necessity arises because the uncertainty in temporal lag increases with smaller temporal lags. The multispectral instruments of Sentinel-2 mission consist of 13 spectral bands. 12 sensor clusters collectively cover a swath of 290 km. Previous studies have mentioned the inter-cluster timing issue in ocean dynamics context such as current and waves (Yurovskaya et al., 2019). Binet et al. (2022b) shows that optical distortion and satellite altitude variations are the two main causes of an important delay's dispersion when using ESA timing table. This effect can produce issues on celerity estimates and up to 10% significant error on bathymetry estimation (errors up to 2–3 m here, Fig. 7) in the coastal zone using wave kinematics methods based on small time differences between satellite images (Poupardin et al., 2016; Almar et al., 2019) or image bands (de Michele et al., 2021; Bergsma et al., 2019b, 2021). That can partially be accounted for by the proposed time-lag correction presented by Binet et al. (2022b) and depending on the latitude, band and sensor, that typically reduces this error down to a few percent.

5. Conclusion

A method of wave tracking using a spatial correlation approach derived from Sentinel-2 was introduced and tested against an Emodnet reference bathymetric survey. The performance is heterogeneous and varies according to the depth range considered and its location. The delivered product seems to be optimal in intermediate waters between 20 and 40 m. However, there is a large dispersion between different scenes. Areas with specific configurations, in this case, the Antioche Channel and the shipping channel at the mouth of the Gironde, appear qualitatively.

Despite continuous improvements, satellite-derived bathymetry assessment from Sentinel-2 currently remains noisy. Here, deviations from the reference bottom can reach 4 to 5 m in the areas where the S2Shores spatial correlation product is most satisfactory here. Because of its noise level, the product is not yet qualified with the CATZOC classification (as a reminder, the CATZOC-C qualification requires that 95% of the probes have a vertical accuracy of less than 2 m + 5% of the water height). An improvement of the accuracy, a filtering on outliers, a proxy of the quality are all necessary for an operational use.

CRediT authorship contribution statement

Rafael Almar: Conceptualization, Writing – original draft. **Erwin W.J. Bergsma:** Conceptualization, Methodology, Writing – original draft. **Grégoire Thoumyre:** Data curation, Software, Validation, Visualization. **Lemai-Chenevier Solange:** Methodology, Project administration, Software, Validation. **Sophie Loyer:** Data curation, Validation. **Stephanie Artigues:** Software, Validation, Visualization. **Grégoire Salles:** Investigation, Methodology. **Thierry Garlan:** Funding acquisition, Project administration, Supervision. **Anne Lifermann:** Funding acquisition, Project administration, Supervision.

Declaration of competing interest

The authors declare that they have no known competing financial interests or personal relationships that could have appeared to influence the work reported in this paper.

Data availability

Data will be made available on request.

Acknowledgment

Research conducted through the project GLOBCOAST ANR-22-ASTR-0013-01.

Appendix A. IHO bathymetry standards S-44 (6th edition)

The IHO S-44 standard is used to qualify hydrographic surveys on the basis of their quality. It describes the orders that are satisfactory for safe navigation. Five different survey orders are defined, each designed to meet different needs: Order 2, Order 1b and 1a, Special Order, and the Exclusive Order. The given criteria define the minimum performance to be achieved for each of the specified orders. The tolerated error ranges are defined for a 95% CI (THU: Total Horizontal Uncertainty, TVU: Total Vertical Uncertainty).

Special Order This is the most stringent order and is intended for use only in areas where underkeel clearance is critical. Because underkeel clearance is critical, a full seabed search is required and the size of the features to be detected by this search is intentionally small. Because under-keel clearance is critical, it is considered unlikely that special order surveys will be conducted in waters deeper than 40 m. Examples of areas that may be special order include moorings, harbors, and critical areas of navigation channels.

Order 1a This order is intended for areas where the sea is so shallow that natural or artificial features of the seabed are visible. where natural or artificial features of the seabed are of concern for the type of surface navigation intended, but where underkeel clearance is less critical than for the special order above. Due to the possible presence of natural or artificial features that may affect surface navigation, a full seabed search is required. due to the possible presence of natural or artificial features that may affect surface navigation, a full seabed search is required, but the size of the feature to be detected is larger than for the special order. larger than for the special order. Under keel clearance becomes less critical with increasing depth. Therefore, the size of the feature to be detected by the full-bottom search increases in areas where the water depth is greater than 40 m. Order 1a surveys may be limited to waters less than 100 m.

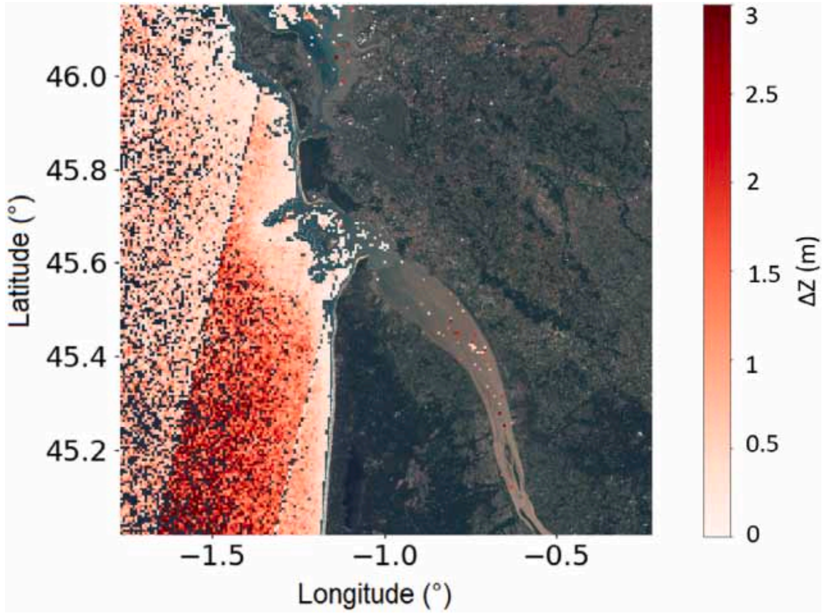

Fig. 7. Difference of bathymetry estimates using ESA sensor cluster handbook timing and reprocessed by Binet et al. (2022b). Sentinel-2 30TXR image on 20200622.

Order 1b This order is intended for areas less than 100 m deep where a general representation of the seabed is considered sufficient for the project. This order is intended for areas less than 100 m deep where a general representation of the seafloor is considered adequate for the type of surface navigation planned in the area. A complete search of the seafloor is not required, which means that some features may be missed, although the maximum line spacing limits the size of features that may not be detected. not detected. This survey sequence is recommended only when underkeel clearance is not considered a problem. is not considered a problem. For example, this is an area where the characteristics of the seabed are such that the likelihood of undetected features is low. characteristics of the seabed are such that the likelihood of the presence of an artificial or natural feature on the seabed that would endanger the type of surface vessel intended to navigate the area is low. endanger the type of surface vessel intended to navigate the area is low.

Order 2 This is the least stringent order and is intended for areas where the water depth is such that a general representation of the sea surface is impossible. is such that a general representation of the sea floor is considered adequate. A complete seafloor survey is not required. It is recommended that Order 2 surveys be limited to areas deeper than 100 m. 100 m, because once the water depth exceeds 100 m, the existence of artificial or natural features large enough to affect the seabed may be compromised. the existence of artificial or natural features large enough to affect surface navigation and yet not detected by an Order 2 survey is considered unlikely.

Appendix B. IHO CATegory Zone Of Confidence (CATZOC) classification

Similar to the S-44 Classification, chartmakers must adhere to international standards that illustrate the quality of the data provided in charts, including the IHO-defined CATegory Zone Of Confidence (CATZOC) classification, which allows mariners to assess the quality of the hydrographic data from which the chart was produced. Since all the information compiled on a chart is derived from data from multiple sources, all individually classified to the S-44 standard, the chart maker combines the information collected through the CATZOC classification (mapping the orders of the S-44 classification and the CATZOC classification). The determination of a Zone of Confidence (or Zone of Reliability: ZOC) is therefore linked to the bathymetric quality of the data used, which must meet 95% of the minimum criteria for depth accuracy, positional accuracy and bottom exploration. The use of the ZOC classification implies the ability to certify that all the conditions in the table below are met. Translating the S-44 standards, the primary concern of a hydrographic surveyor is in areas of shallow or relatively shallow water up to 40 m depth. At these depths, there is an increased risk of marine casualties resulting in marine and coastal environmental disasters affecting the maritime economies of all affected states. For this reason, the most demanding category of surveys is defined as Special Order (SO) surveys and must be conducted in coastal areas where underwater clearance is critical to safe navigation.

The new edition of the S-44 standard (edition 6.0.0, September 2020, Belmonte, 2020) proposes a classification matrix allowing to extend the data qualification to other types of surveys not dedicated to navigation safety. The 5 orders defined previously remain and the reference of the selected cells is sufficient to define if a survey remains classifiable according to one of these orders. Here are some clarifications on the interpretation of the S-44 matrix:

Bathymetric coverage This criterion corresponds to the quantification of the area covered by the measurement technique = surface area/total area: 100% means complete coverage (i.e. no coverage hole in the product, which must have a continuous surface over the measurement area) and 200% = double coverage (i.e. twice everywhere).

Feature detection It determines the ability of a system to detect features of a defined size. In general, an object is considered detectable when it has been characterized with several concordant measurements. The resolution is therefore necessarily lower than that of the system. Or, in the case of a composite product, it would be necessary to be able to certify that it has been detected on each of the images taken individually before they are merged into the composite. To be distinguished from "feature search": this criterion corresponds to the quantification of the area scanned using a systematic method of feature identification. This corresponds to the features identified during the survey that are resurveyed to characterize them in more detail (either with the same measurement system but on dedicated profiles and by increasing the resolution of the system — or with a side-scan sonar). This criterion cannot be considered in the case of satellite-derived bathymetry.

References

Abessolo, G.O., Almar, R., Bonou, F., Bergsma, E., 2020. Error proxies in video-based depth inversion: Temporal celerity estimation. J. Coast. Res. 95 (SI), 1101–1105.

Almar, R., Bergsma, E.W., Catalan, P.A., Cienfuegos, R., Suarez, L., Lucero, F., Lerma, A.N., Desmazes, F., Perugini, E., Palmsten, M.L., et al., 2021a. Sea state from single optical images: A methodology to derive wind-generated ocean waves from cameras, drones and satellites. Remote Sens. 13 (4), 679.

Almar, R., Bergsma, E.W., Gawehn, M., Aarninkhof, S., Benshila, R., 2020. High-frequency temporal wave-pattern reconstruction from a few satellite images: A new method towards estimating regional bathymetry. J. Coast. Res. 95 (SI), 996–1000.

Almar, R., Bonneton, P., Senechal, N., Roelvink, D., 2009. Wave celerity from video imaging: A new method. In: Coastal Engineering 2008: (in 5 Volumes). World Scientific, pp. 661–673.

Almar, R., Kestenare, E., Boucharel, J., 2019. On the key influence of remote climate variability from Tropical Cyclones, North and South Atlantic mid-latitude storms on the Senegalese coast (West Africa). Environ. Res. Commun. 1 (7), 071001.

Almar, R., Michallet, H., Cienfuegos, R., Bonneton, P., Tissier, M., Ruessink, G., 2014. On the use of the Radon Transform in studying nearshore wave dynamics. Coast. Eng. 92, 24–30.

Almar, R., Ranasinghe, R., Bergsma, E.W., Diaz, H., Melet, A., Papa, F., Vousdoukas, M., Athanasiou, P., Dada, O., Almeida, L.P., et al., 2021b. A global analysis of extreme coastal water levels with implications for potential coastal overtopping. Nat. Commun. 12 (1), 1–9.

Almar, R., Stieglitz, T., Addo, K.A., Ba, K., Ondoa, G.A., Bergsma, E.W., Bonou, F., Dada, O., Angnuureng, D., Arino, O., 2022. Coastal zone changes in West Africa: Challenges and opportunities for satellite earth observations. Surv. Geophys. 1–27.

Baba, M.W., Thoumyre, G., Bergsma, E.W., Daly, C.J., Almar, R., 2021. Deriving large-scale coastal bathymetry from Sentinel-2 images using an High-Performance Cluster: A case study covering North Africa's coastal zone. Sensors 21 (21), 7006.

Belmonte, I., 2020. Iho file no. s3/8151 & s3/7198 & s3/3061 circular letter n ° 33.

Benveniste, J., Cazenave, A., Vignudelli, S., Fenoglio-Marc, L., Shah, R., Almar, R., Andersen, O., Birol, F., Bonnefond, P., Bouffard, J., et al., 2019. Requirements for a coastal hazards observing system. Front. Mar. Sci. 6, 348.

Bergsma, E.W., Almar, R., 2018. Video-based depth inversion techniques, a method comparison with synthetic cases. Coast. Eng. 138, 199–209.

Bergsma, E.W., Almar, R., 2020. Coastal coverage of ESA' Sentinel 2 mission. Adv. Space Res. 65 (11), 2636–2644. http://dx.doi.org/10.1016/j.asr.2020.03.001.

Bergsma, E.W., Almar, R., de Almeida, L.P.M., Sall, M., 2019a. On the operational use of UAVs for video-derived bathymetry. Coast. Eng. 152, 103527.

Bergsma, E.W., Almar, R., Giros, A., Lemai-Chenevier, S., Thoumyre, G., Artigues, S., Garlan, T., Degoul, R., 2022. S2shores: A python library for estimating coastal bathymetry. Coast. Eng. Proc. (37), 36.

Bergsma, E.W., Almar, R., Maisongrande, P., 2019b. Radon-augmented sentinel-2 satellite imagery to derive wave-patterns and regional bathymetry. Remote Sens. 11 (16), 1918.

Bergsma, E.W., Almar, R., Rolland, A., Binet, R., Brodie, K.L., Bak, A.S., 2021. Coastal morphology from space: A showcase of monitoring the topography-bathymetry continuum. Remote Sens. Environ. 261, 112469. http://dx.doi.org/10.1016/j.rse.2021.112469.

Binet, R., Bergsma, E., Poulain, V., 2022a. Accurate sentinel-2 inter-band time delays. ISPRS Ann. Photogramm., Remote Sens. Spatial Inf. Sci. V-1-2022, 57–66. http://dx.doi.org/10.5194/isprs-annals-V-1-2022-57-2022.

Binet, R., Bergsma, E., Poulain, V., 2022b. Accurate sentinel- 2 inter-band time delays. ISPRS Ann. Photogramm., Remote Sens. Spatial Inf. Sci. 1, 57–66.

Caballero, I., Stumpf, R.P., 2020. Towards routine mapping of shallow bathymetry in environments with variable turbidity: Contribution of Sentinel-2A/B satellites mission. Remote Sens. 12 (3), 451.

Caballero, I., Stumpf, R., 2023. Confronting turbidity, the major challenge for satellite-derived coastal bathymetry. Sci. Total Environ. 161898.

Cahalane, C., Magee, A., Monteys, X., Casal, G., Hanafin, J., Harris, P., 2019. A comparison of Landsat 8, RapidEye and Pleiades products for improving empirical predictions of satellite-derived bathymetry. Remote Sens. Environ. 233, 111414.

Cesbron, G., Melet, A., Almar, R., Lifermann, A., Tullot, D., Crosnier, L., 2021. Pan-european satellite-derived coastal bathymetry-review, user needs and future services. Front. Mar. Sci. 1591.

Chénier, R., Ahola, R., Sagram, M., Faucher, M.-A., Shelat, Y., 2019. Consideration of level of confidence within multi-approach satellite-derived bathymetry. ISPRS Int. J. Geo-Inf. 8 (1), 48.

Cox, C., Munk, W., 1954. Measurement of the roughness of the sea surface from photographs of the sun's glitter. Josa 44 (11), 838–850.

Daly, C., Baba, W., Bergsma, E., Thoumyre, G., Almar, R., Garlan, T., 2022. The new era of regional coastal bathymetry from space: A showcase for West Africa using optical Sentinel-2 imagery. Remote Sens. Environ. 278, 113084.

de Michele, M., Raucoules, D., Idier, D., Smai, F., Foumelis, M., 2021. Shallow bathymetry from multiple sentinel 2 images via the joint estimation of wave celerity and wavelength. Remote Sens. 13 (11), 2149.

Holman, R., Bergsma, E.W., 2021. Updates to and performance of the cbathy algorithm for estimating nearshore bathymetry from remote sensing imagery. Remote Sens. 13 (19), 3996.

Holman, R.A., Brodie, K.L., Spore, N.J., 2017. Surf zone characterization using a small quadcopter: Technical issues and procedures. IEEE Trans. Geosci. Remote Sens. 55 (4).

Kudryavtsev, V., Yurovskaya, M., Chapron, B., Collard, F., Donlon, C., 2017. Sun glitter imagery of ocean surface waves. Part 1: Directional spectrum retrieval and validation. J. Geophys. Res.: Oceans 122 (2), 1369–1383.

Kurniawan, A., Pranowo, W.S., Prihanto, Y., Bastari, A., Setiyadi, J., 2021. Challenges of acquisition bathymetry information on PlanetScope data and nautical chart: Experiment based on IHO S-44 total vertical uncertainty in multi-method satellite-derived bathymetry. J. Hunan Univ. Nat. Sci. 48 (12).

Laporte, J., Coulibaly, F., 2019. An ESA project: Sentinel coastal charting worldwide and other SDB applications. In: OCEANS 2019-Marseille. IEEE, pp. 1–6.

Laporte, J., Dolou, H., Avis, J., Arino, O., 2020. Thirty years of satellite derived bathymetry: The charting tool that hydrographers can no longer ignore. Int. Hydrogr. Rev. 25, 129–154.

Lyzenga, D.R., Malinas, N.P., Tanis, F.J., 2006. Multispectral bathymetry using a simple physically based algorithm. IEEE Trans. Geosci. Remote Sens. 44 (8), 2251–2259.

Matsumoto, Y., 2016. Satellite derived bathymetry: toward utilisation for hydrographic services.

Mavraeidopoulos, A.K., Pallikaris, A., Oikonomou, E., 2017. Satellite derived bathymetry (SDB) and safety of navigation. In: The International Hydrographic Review.

Melet, A., Teatini, P., Le Cozannet, G., Jamet, C., Conversi, A., Benveniste, J., Almar, R., 2020. Earth observations for monitoring marine coastal hazards and their drivers. Surv. Geophys. 41 (6), 1489–1534.

Nicolas, K.M., Drumetz, L., Lefèvre, S., Tiede, D., Bajjouk, T., Burnel, J.-C., 2023. Deep learning–based bathymetry mapping from multispectral satellite data around Europa Island. In: European Spatial Data for Coastal and Marine Remote Sensing. Springer, pp. 97–111.

Pike, S., Traganos, D., Poursanidis, D., Williams, J., Medcalf, K., Reinartz, P., Chrysoulakis, N., 2019. Leveraging commercial high-resolution multispectral satellite and multibeam sonar data to estimate bathymetry: The case study of the Caribbean Sea. Remote Sens. 11 (15), 1830.

Poupardin, A., Idier, D., de Michele, M., Raucoules, D., 2016. Water depth inversion from a single SPOT-5 dataset. IEEE Trans. Geosci. Remote Sens. 54 (4), 2329–2342. http://dx.doi.org/10.1109/TGRS.2015.2499379.

Sentinel, E., 2015. User Handbook. ESA Standard Document 64.

Thierry, S., Dick, S., George, S., Benoit, L., Cyrille, P., 2019. EMODnet Bathymetry a compilation of bathymetric data in the European waters. In: OCEANS 2019-Marseille. IEEE, pp. 1–7.

Thoumyre, G., Bergsma, E., Almar, R., Giros, A., Lemai-Chenevier, S., Artigues, S., Garlan, T., 2023. A New Python Tool for Coastal Bathymetry Estimation: S2Shores. Technical Report, Copernicus Meetings.

Thuan, D.H., Almar, R., Marchesiello, P., Viet, N.T., 2019. Video sensing of nearshore bathymetry evolution with error estimate. J. Mar. Sci. Eng. 7 (7), 233.

Tissier, M., Bonneton, P., Almar, R., Castelle, B., Bonneton, N., Nahon, A., 2011. Field measurements and non-linear prediction of wave celerity in the surf zone. Eur. J. Mech. B Fluids 30 (6), 635–641.

Yurovskaya, M., Kudryavtsev, V., Chapron, B., Collard, F., 2019. Ocean surface current retrieval from space: The Sentinel-2 multispectral capabilities. Remote Sens. Environ. 234, 111468.